

# Fisher Information and Steric Effect: Study of the Internal Rotation Barrier of Ethane

Rodolfo O. Esquivel,<sup>\*,†,§</sup> Shubin Liu,<sup>\*,⊥</sup> Juan Carlos Angulo,<sup>‡,§</sup> Jesús S. Dehesa,<sup>‡,§</sup> Juan Antolín,<sup>§,||</sup> and Moyocoyani Molina-Espíritu<sup>†</sup>

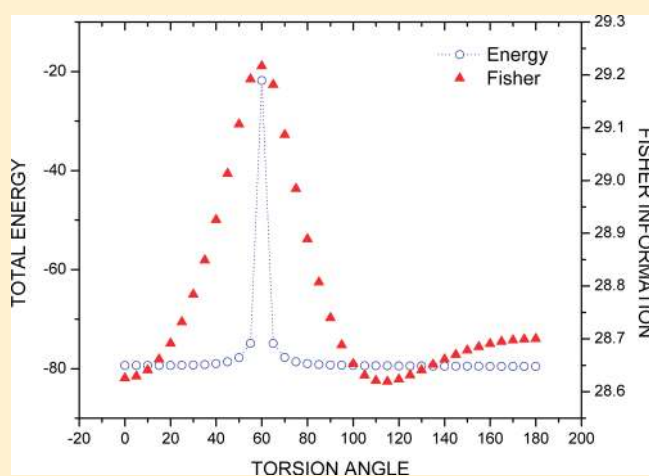
<sup>†</sup>Departamento de Química, Universidad Autónoma Metropolitana, 09340 México D.F., México

<sup>‡</sup>Departamento de Física Atómica, Molecular y Nuclear and <sup>§</sup>Instituto Carlos I de Física Teórica y Computacional, Universidad de Granada, 18071 Granada, Spain

<sup>⊥</sup>Research Computing Center, University of North Carolina, Chapel Hill, North Carolina 27599-3420, United States

<sup>||</sup>Departamento de Física Aplicada, EUITIZ, Universidad de Zaragoza, 50018-Zaragoza, Spain

**ABSTRACT:** On the basis of a density-based quantification of the steric effect [Liu, *S. B. J. Chem. Phys.* **2007**, *126*, 244103], the origin of the internal rotation barrier between the eclipsed and staggered conformers of ethane is systematically investigated in this work from an information-theoretical point of view by using the Fisher information measure in conjugated spaces. Two kinds of computational approaches are considered in this work: adiabatic (with optimal structure) and vertical (with fixed geometry). The analyses are performed systematically by following, in each case, the conformeric path by changing the dihedral angle from 0 to 180°. This is calculated at the HF, MP2, B3LYP, and CCSD(T) levels of theory and with several basis sets. Selected descriptors of the densities are utilized to support the observations. Our results show that in the adiabatic case the eclipsed conformer possesses a larger steric repulsion than the staggered conformer, but in the vertical cases the staggered conformer retains a larger steric repulsion. Our results verify the plausibility for defining and computing the steric effect in the post-Hartree–Fock level of theory according to the scheme proposed by Liu.



## 1. INTRODUCTION

Notwithstanding the Fisher information of a probability distribution was introduced in the early decades of the past century,<sup>1</sup> its utility has been assessed until recently for the informational description of atoms,<sup>2,3</sup> molecules,<sup>4</sup> and processes<sup>5</sup> among others. Its appealing features differ appreciably from other information measures because of its *local* character,<sup>9</sup> in contrast with the *global* nature of several functionals, such as the variance or the Shannon,<sup>6</sup> Tsallis,<sup>7</sup> and Rényi<sup>8</sup> entropies. Besides, since Fisher information is defined as a functional of the distribution gradient, its local character provokes an enhanced sensitivity even over a very small-sized region in the domain of definition of the distribution, as will be described below. This is in contrast to global information measures such as the Shannon entropy, disequilibrium, or variance, whose values are conditioned by the behavior of the density over the whole domain, hence displaying much lesser variations to local changes on the distribution.<sup>10</sup> Interestingly, an analytical relationship between the densities of the Shannon entropy and Fisher information for atomic and molecular systems has been recently established.<sup>11</sup>

Fisher information has been employed for the interpretation of different physical and chemical phenomena within an information-theoretical framework, mainly for atomic and molecular systems and processes (e.g., ionization, reactions), among others. Moreover, Fisher information constitutes an essential component of “complexity measures”,<sup>12</sup> a topic of research that has attracted attention because of its special features for quantifying the level of localization or organization of the considered distribution. Such is the case, for instance, of the recently introduced “Fisher–Shannon”<sup>3</sup> and “Cramér–Rao”<sup>12</sup> complexities and their corresponding information planes, where concepts such as randomness and uncertainty are employed. Recent applications of these complexities to atomic systems can be found in ref 13.

Furthermore, through the concept of Fisher information it has been possible to introduce functionals which allow establishing

**Received:** October 4, 2010

**Revised:** February 9, 2011

**Published:** April 07, 2011

useful *local* comparative measures between two different densities. Such is the case of the so-called “relative Fisher information”,<sup>14</sup> analogous to the “Kullback–Leibler” relative entropy for the Shannon case,<sup>15</sup> and more recently the “Fisher divergence”,<sup>16</sup> which represents a symmetrized form of the relative Fisher information, stressing the *local* features of the distribution in contrast with the “Jensen–Shannon divergence”,<sup>17</sup> which only emphasizes its *global* character.

In recent years there has been an increasing interest for analyzing the electronic structure of atoms and molecules by applying information theory (IT).<sup>18</sup> For the molecular cases, these studies have shown that information-theoretical measures are capable of providing simple pictorial chemical descriptions of the processes they exert through the localized/delocalized behavior of the electron densities in position and momentum spaces. In a recent study,<sup>19</sup> we have provided evidence which supports the utility of the information-theoretical measures in position and momentum spaces to detect the transition state and the stationary points of elementary chemical reactions to reveal the bond-breaking/bond-forming regions of the simplest hydrogen abstraction and the identity S<sub>N</sub>2 exchange chemical processes. Besides, we have shown that Shannon entropies are capable of explaining the synchronous/asynchronous behavior of the mechanistic course of the above-mentioned reactions.<sup>20</sup> Moreover, the utility of the Fisher information measure has been also assessed to detect the transition state and the stationary points for the same elementary reactions mentioned above.<sup>21</sup> Further, a very recent study on molecular complexities has shown that information measures and planes are able to detect not only randomness or localization but also pattern and organization.<sup>22</sup> To the best of our knowledge, no information-theoretical studies have been reported on the internal rotational barrier for molecules.

On the verge of comprehension of the origin of internal rotational barriers,<sup>23</sup> it is essential to understand molecular conformational changes, which are at the heart of fundamental topics in chemistry and biology such as protein folding/misfolding,<sup>24</sup> signal transduction cascades<sup>25</sup> in cells, and chemical reactivity for individual molecules (regio-, diastereo-, and enantioselectivity). Nevertheless, there still exists great controversy over the origin of the internal rotational barrier even for as simple a molecule as ethane.<sup>26</sup> The main controversy lies in attributing different amounts of steric, electrostatic, and hyperconjugation quantum effects to the barrier height. The steric effect is an essential concept in chemistry, biochemistry, and pharmacology, affecting rates and energies of chemical reactions, impacting structure, dynamics, and function of enzymes, and governing to a degree how and at what rate a drug molecule interacts with a receptor. This important effect originates from the fact that atoms in molecules occupy a certain amount of space, and also when atoms are brought together, then hindrance will be necessarily induced, resulting in changes in shape, energy, and reactivity. However, there is no general agreement in the literature on how to uniquely quantify this effect. Recently, a density-based quantification of the steric and quantum effects has been proposed by one of the authors.<sup>27</sup> Within this energy partition scheme, the total energy density functional is decomposed into three independent contributions from steric, electrostatic, and quantum effects under the framework of density functional theory (DFT). Liu<sup>27</sup> and later Nagy<sup>28</sup> have identified the steric component with the Weizsäcker kinetic energy, noticing an intrinsic relationship between the Fisher information and

the steric energy. This approach has been investigated at the atomic and functional group levels<sup>29</sup> and applied to examine the internal rotation barriers of ethane and *n*-butane,<sup>30</sup> for molecules with one rotatable dihedral angle<sup>31</sup> and also for the S<sub>N</sub>2 reaction.<sup>32</sup>

On the considerations above we have conducted this work from the perspective of the information-theoretical measure of Fisher<sup>1</sup> to investigate the internal rotational barrier for ethane. The goals of the study are 2-fold: (i) to investigate the origin of the internal rotation barrier between the eclipsed and staggered conformers of ethane with emphasis in analyzing the steric effect according to the density-based quantification scheme proposed by Liu,<sup>27</sup> and (ii) to test this scheme in assessing the dependence of the calculated steric energy on the choice of the level of theory; i.e., since the new definition only depends on the densities and their gradients to calculate the steric effect<sup>27</sup> it appears worthy of belief that the extension of the approach to post-Hartree–Fock and DFT methods should be straightforward.

## 2. THEORETICAL DETAILS

The central quantities under study are the Fisher information

$$I_r = \int \frac{|\bar{\nabla}\rho(\vec{r})|^2}{\rho(\vec{r})} d^3r \quad (1)$$

in position space and similarly

$$I_p = \int \frac{|\bar{\nabla}\gamma(\vec{p})|^2}{\gamma(\vec{p})} d^3p \quad (2)$$

in momentum space, where  $\rho(\vec{r})$  and  $\gamma(\vec{p})$  denote the normalize-to-unity electron density distributions in the position and momentum spaces, respectively. The total electron density of a molecule, in the independent particle approximation, consists of a sum of contributions from electrons in occupied orbitals. Thus, in momentum space, the contribution from an electron in a molecular orbital  $\phi_i(\vec{p})$  to the total electron density is given by  $|\phi_i(\vec{p})|^2$ . The orbitals  $\phi_i(\vec{p})$  are then related by Fourier transforms to the corresponding orbitals in position space  $\psi_i(\vec{r})$ . Standard procedures for the Fourier transformation of position space orbitals generated by ab initio methods have been described.<sup>33</sup> The orbitals employed in ab initio methods are linear combinations of atomic basis functions, and since analytic expressions are known for the Fourier transforming of such basis functions,<sup>34</sup> the transformation of the total molecular electronic wave function from position to momentum space is computationally straightforward.<sup>35</sup>

In contrast to the Shannon entropy, which is a global spreading measure of the electron density, the position Fisher information is closely connected to the kinetic energy<sup>36</sup> due to its dependence on the gradient of the distribution thus emphasizing its local character; i.e., it measures the spatial pointwise concentration of the electronic probability cloud and quantifies the gradient content of the electron distribution, hence revealing the irregularities of the density and providing a quantitative estimation of its fluctuations. Besides, according to the localized/delocalized features of the distributions, Fisher also measures the departure of the probability density from *disorder*.<sup>1,9</sup> A similar interpretation follows for the momentum Fisher information. Moreover, the position Fisher information and momentum Fisher information are reciprocal measures that satisfy the

**Table 1. Total Energies (au) for Staggered and Eclipsed Conformers of Ethane and Their Energy Differences (kcal/mol) at Different Levels of Theory**

method	staggered <sup>a</sup>	eclipsed		energy difference	
		adiabatic	staggered <sup>b</sup>	adiabatic	vertical
B3LYP/aug-cc-PVDZ	-79.836 082	-79.831 761	-79.831 509	2.71	2.87
B3LYP/6-311++G**	-79.856 575	-79.852 268	-79.851 864	2.70	2.96
CCSD(T)/aug-cc-PVDZ	-79.597 789	-79.593 339	-79.592 861	2.79	3.09
CCSD(T)/6-311++G**	-79.616 591	-79.611 857	-79.611 601	2.97	3.13
MP2/aug-cc-PVDZ	-79.551 122	-79.546 313	-79.546 064	3.02	3.17
MP2/6-311++G**	-79.571 672	-79.566 764	-79.566 445	3.08	3.28
HF/aug-cc-PVDZ	-79.237 278	-79.232 129	-79.231 613	3.23	3.55
HF/6-311++G**	-79.251 935	-79.247 063	-79.246 089	3.06	3.67

<sup>a</sup> Staggered conformation in the optimized geometry. <sup>b</sup> Eclipsed conformation in the staggered geometry.

uncertainty relation  $I_r I_p \geq 4n^2$  for  $n$ -dimensional quantum systems.<sup>37</sup> For three-dimensional systems they fulfill the inequality  $I_r I_p \geq 36$ .

An interesting aspect of Fisher information is linked to the Weiszäcker kinetic energy:<sup>38</sup>

$$T_w[\rho] = \frac{N}{8} \int \frac{|\nabla \rho(\vec{r})|^2}{\rho(\vec{r})} d^3r \quad (3)$$

with the number of electrons  $N$  arising from the normalization of the electron density. Equation 3 is in turn linked to the density-based quantification of the steric energy  $E_S[\rho]$ , see eq 6 in ref 22, according to which  $E_S[\rho]$  is a measure of the intrinsic dimensions upheld by the system with the contributions from other effects, e. g., quantum and electrostatic, completely excluded.

Regarding the behavior of Fisher information, Nagy<sup>28</sup> has pointed out that, for a normal distribution,  $I$  is equal to the inverse variance  $V$  in Cramér–Rao’s inequality ( $IV \geq n^2$ ) with  $n$  being the space dimensionality.<sup>9,10,39</sup> In this case a narrower distribution (a density that extends to a small portion in the space) has a larger Fisher information. On the other hand, if the density fills a large volume in space the Fisher information is small. Even though atoms and molecules do not possess normal distributions, still Cramér–Rao’s inequality holds, and Fisher information represents a measure of the “narrowness” of a distribution, meaning that the steric energy proposition<sup>27</sup> can be supported by information-theoretical arguments.

With the purpose of characterizing the Fisher information of the conformers of ethane, we have computed several reactivity properties such as the total dipole moment, the hardness ( $\eta$ ), and the electrophilicity index ( $\omega$ ). These properties were obtained at the Hartree–Fock level of theory (HF) in order to employ the Koopmans theorem,<sup>40</sup> for relating the first vertical ionization energy and the electron affinity to the highest occupied molecular orbital (HOMO) and lowest unoccupied molecular orbital (LUMO) energies, which are necessary to calculate the conceptual DFT properties. The hardness ( $\eta$ ) is obtained within this framework<sup>41</sup> through

$$\eta = \frac{1}{S} \sim \frac{\varepsilon_{\text{LUMO}} - \varepsilon_{\text{HOMO}}}{2} \quad (4)$$

where  $\varepsilon$  denotes the frontier molecular orbital energies and  $S$  is the softness of the system. It is worth mentioning that the factor 1/2 in eq 4 was put originally to make the hardness definition symmetrical with respect to the chemical potential<sup>42</sup>

$$\mu = \left( \frac{\partial E}{\partial N} \right)_{\mu(\tau)} = \frac{\varepsilon_{\text{LUMO}} + \varepsilon_{\text{HOMO}}}{2} \quad (5)$$

although it has been recently disowned.<sup>43</sup> In general terms, the chemical hardness and softness are good descriptors of chemical reactivity. The former has been employed<sup>43,44</sup> as a measure of the reactivity of a molecule in the sense of the resistance to changes in the electron distribution of the system; i.e., molecules with larger values of  $\eta$  are interpreted as being the lesser reactive ones. In contrast, the  $S$  index quantifies the polarizability of the molecule<sup>45</sup> and hence soft molecules are more polarizable and possess a predisposition to acquiring additional electronic charge.<sup>46</sup> The chemical hardness  $\eta$  is a central quantity for use in the study of reactivity through the hard and soft acids and bases principle.<sup>47</sup>

The electrophilicity index,<sup>48</sup>  $\omega$ , allows a quantitative classification of the global electrophilic nature of a molecule within a relative scale. The electrophilicity index of a system in terms of its chemical potential and hardness is given by the expression

$$\omega = \frac{\mu^2}{2\eta} \quad (6)$$

The electrophilicity is also a good descriptor of chemical reactivity, which quantifies the global electrophilic power of the molecules (predisposition to acquire an additional electronic charge).<sup>46</sup>

### 3. RESULTS AND DISCUSSION

This study is performed by tracking the conformeric path of the internal rotation angle of ethane. The strategy for the calculations takes into account two categories: adiabatic (i.e., optimized geometry) and vertical (i.e., fixed geometry). In the first case, both staggered and eclipsed conformers are in their respective optimized structure, whereas in the latter situation bond lengths and angles for the two conformers are fixed to be identical except for the changing dihedral angle. For the adiabatic series, each time the dihedral angle of the two conformers is altered, a geometric optimization with the fixed dihedral angle will be performed for both conformers. For the vertical category, two cases are considered in this work. In the first case, we use the optimized eclipsed conformer as the reference and attain the staggered conformer by rotating the dihedral angle from 0 to 180°. In the second case, we employ the optimized geometry of

**Table 2.** Steric Energies (au) (Obtained by Use of eq 3) for Staggered and Eclipsed Conformers of Ethane and Steric Energy Differences (kcal/mol) at Different Levels of Theory

method	staggered <sup>a</sup>	eclipsed		steric energy difference	
		adiabatic	staggered <sup>b</sup>	adiabatic	vertical
B3LYP/aug-cc-PVDZ	64.273 716	64.278 574	64.268 906	3.05	−3.02
B3LYP/6-311++G**	64.245 620	64.251 691	64.238 814	3.81	−4.27
CCSD(T)/aug-cc-PVDZ	64.575 113	64.577 781	64.569 175	1.67	−3.73
CCSD(T)/6-311++G**	64.527 896	64.538 168	64.522 067	6.45	−3.66
MP2/aug-cc-PVDZ	64.574 872	64.578 404	64.569 175	2.22	−3.57
MP2/6-311++G**	64.530 909	64.535 261	64.522 067	2.73	−5.55
HF/aug-cc-PVDZ	64.581 453	64.585 931	64.566 387	2.81	−9.45
HF/6-311++G**	64.534 322	64.538 753	64.518 597	2.78	−9.87

<sup>a</sup> Staggered conformation in the optimized geometry. <sup>b</sup> Eclipsed conformation in the staggered geometry.

the staggered conformer as the starting structure and the eclipsed conformer is obtained from it by changing the dihedral angle from 180 to 0°. For both vertical cases, no structural optimization is carried out. The dihedral angle considered for ethane is  $\angle\text{H}-\text{C}-\text{C}-\text{H}$  and the interval is 5°. Thus, we will examine densities obtained at HF, DFT-B3LYP levels and post-HF ones, MP2 and CCSD(T). We will examine Pople's<sup>49</sup> 6-311+G\* and 6-311++G\*\* and Dunning's correlation consistent basis set, aug-cc-pVDZ.<sup>50</sup> The electronic structure calculations were carried out with the Gaussian 03 suite of programs.<sup>51</sup> The molecular Fisher information measures in position and momentum spaces for the conformeric structures described above were obtained by employing software developed in our laboratory along with three-dimensional numerical integration routines<sup>52</sup> and the DGRID suite of programs.<sup>35</sup> DFT parameters, the hardness and electrophilicity, were calculated by use of eqs 4 and 6 and the standard hybrid B3LYP functional.<sup>51</sup> Atomic units are employed throughout the study except for the total and steric energy differences (kilocalories per mole) and the dipole moment (debyes).

**3.1. Total and Steric Energies.** To investigate the plausibility of defining and computing the steric effect in the post-Hartree–Fock level of theory and assessing its impact on the steric energy, we have tabulated the total and the steric energies in Tables 1 and 2, respectively, for the aforementioned methods and basis sets. In Table 1 the total energies for the staggered and eclipsed conformations of ethane at different levels of theory are shown. The adiabatic and vertical energy differences (eclipsed–staggered) between the two conformers are also included in Table 1. As discussed in the preceding paragraph, two vertical comparisons are possible: one using the staggered conformer as the reference and the other using the eclipsed structure. In Tables 1 and 2 we only illustrate the case for the staggered geometry as a reference because it possesses the lowest total energy. With each conformer of ethane in the optimized geometry, the adiabatic energy difference gives a positive quantity for all methods, indicating that the eclipsed conformer possesses a larger steric repulsion than the staggered conformer, which is consistent with the chemical intuition. In addition, it is observed that the total energy differences are similar for all calculations in both the adiabatic and the vertical cases, with consistently larger energies for the vertical one as observed for all methods, an observation that is due to the geometry constraints imposed onto the vertical choice by fixing the internal angles and distances

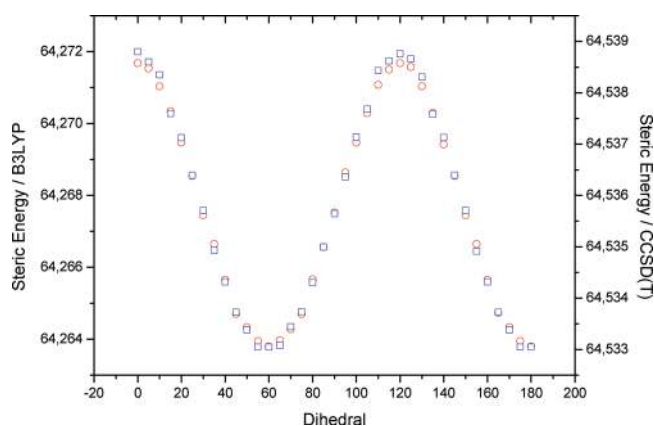


**Figure 1.** Comparison of the steric energy at the B3LYP (red open circles) and CCSD(T) (blue open squares) levels of theory in a 6-311+G\* basis set for the adiabatic conformations of ethane.

when the torsion angle reaches the eclipsed conformation, hence the augment on the energy. This is in agreement with a previous study<sup>30</sup> performed at the HF and DFT levels for the same system. Note that all methods show the same trends and that the energy differences are increasingly larger for B3LYP, CCSD, MP2, and HF.

Table 2 shows the steric energy, calculated by use of eq 3, for the staggered and eclipsed conformations of ethane at different levels of theory along with the adiabatic and vertical energy differences (eclipsed–staggered) between the two conformers. As observed in Table 1, with each conformer of ethane in the optimized geometry, the steric energy difference for the adiabatic case yields a positive quantity for all methods, indicating the well-known fact that the eclipsed conformer holds a larger steric repulsion than the staggered conformer. In contrast, for the vertical cases where bond distances and angles take either the staggered or eclipsed values, the steric energy differences become negative for all methods, showing that the staggered conformer holds a larger steric repulsion than its eclipsed counterpart. This is not reflected in the total energy differences (Table 1), which are all positive, but in the steric energy ones where the hindrance impediment becomes important, i.e., the neglecting of the electronic interactions by constraining the geometry in the vertical case (no relaxing effects), the nuclear interactions become more important in the staggered conformation than in



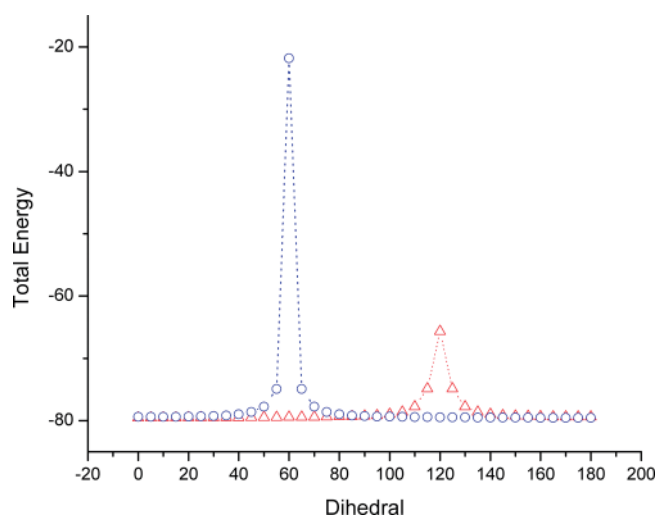


**Figure 2.** Total energy (au) for the eclipsed (red open triangles) and staggered (blue open circles) conformations of ethane as the references in the vertical case.

the eclipsed one. These observations are again in agreement with previous work,<sup>30</sup> and this is in accordance with our plausibility argument (see above) with respect to employing post-Hartree–Fock methods to compute steric energies as may be observed from Table 2.

To emphasize the above and provide a visual confirmation of the extension of the density-based quantification approach<sup>27</sup> to post-Hartree–Fock and DFT methods, we have depicted in Figure 1 a comparison of the steric energy between the B3LYP and CCSD(T) levels of theory in a 6-311+G\* basis set for the adiabatic conformations for ethane.

### 3.2. Vertical Conformer Cases. 3.2.1. Eclipsed Conformer.

In this section we consider the two vertical cases (eclipsed and staggered) where the conformers are constrained to fixed bond lengths and angles according to the eclipsed or staggered optimized structure and then vary the internal dihedral angle to obtain the conformeric path for each case. All of them were calculated at the MP2/aug-ccPVDZ level of theory for the energies and for the Fisher information measures and at the B3LYP/aug-ccPVDZ level for the reactivity parameters. Densities were calculated with a relative error of  $10^{-5}$  for the numerically approximated integrations.

The total energies for both the staggered and the eclipsed conformations are depicted in Figure 2 at the MP2/aug-ccPVDZ level of theory, where the conformeric structures were obtained in each case by constraining the geometry to that of the optimized eclipsed/staggered conformer (as the reference) to attain the staggered/eclipsed conformeric structure by varying the dihedral angle from 0 to 180° and from 180 to 0°, respectively. As observed in Figure 2, the energies remain fairly constant when the torsion angle varies up to a point where the energies are maxima at 60° for the staggered and 120° for the eclipsed reference conformations; then the eclipsed conformeric structure is attained for the former and the staggered one for the latter as the angle augments/diminishes. To understand the energy changes observed in Figure 2, we recall the imposed geometry constraints which, in the absence of other electronic effects arising from the relaxation of the structures, cause the hindrance impediment to be more important in the staggered

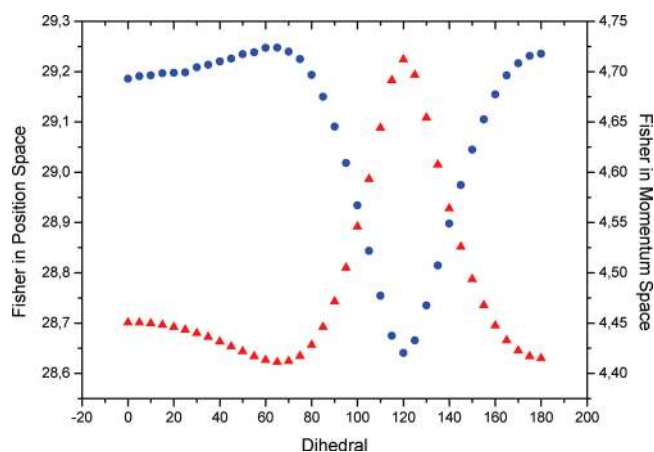


**Figure 3.** Fisher information in conjugated spaces (position space in red triangles; momentum space in blue circles) for the eclipsed conformation of ethane as the reference in the vertical case.

conformation (on the order of 60 au) than in the eclipsed one (on the order of 15 au) due to the nuclear interactions; i.e., in the former each hydrogenic atom is much more exposed to the rest than in the latter case.

Fisher information in position space and Fisher information in momentum space are depicted in Figure 3 at the MP2/aug-ccPVDZ level of theory. It may be noted from Figure 3 that they behave in an opposite manner in accordance with the Heisenberg principle, i.e., Fisher information in position space shows a local minimum at around 60° and a very pronounced maximum at 120°, and the opposite is observed for the momentum space quantity. Interestingly, both quantities possess richer structure compared with the energy (see Figure 2). Concerning the localized/delocalized behavior of the conjugated space densities, we have performed elsewhere<sup>53</sup> an information-theoretical analysis of the Shannon entropies in conjugated spaces. In position space, two kinds of structures can be characterized at the extrema of the constrained path for the conformeric eclipsed geometry; i.e., the staggered conformer holds a high delocalized density at 60°, whereas the eclipsed conformation possesses a highly localized density at 120°. In accordance with these features is that Fisher in position space is able to measure the “narrowness” of the distributions; i.e., we observe from Figure 3 that a localized density (squeezed) corresponds to larger values of the Fisher measure whereas a delocalized distribution (less compressed) is associated with smaller values of its gradient. Accordingly, as a result the staggered conformation constrained to the eclipsed geometry is less “compressed” and the eclipsed one is more “squeezed”; therefore the influence from the steric effect is more pronounced in the eclipsed conformer. The situation for the momentum space quantities is the opposite; i.e., according to the Shannon entropy study<sup>53</sup> the staggered conformation shows a localized momentum density (low kinetic energy) whereas a delocalized density in momentum space is shown for the eclipsed conformation (high kinetic energy) and this is reflected by the Fisher information quantities as may be observed from Figure 3 in that a narrow momentum density is observed for the staggered conformation compared to the eclipsed one, which shows a lesser squeezed density. This behavior altogether shows a picture where the steric effect is shown to be more pronounced for the eclipsed conformer with a higher kinetic energy and lesser compressed momentum density. A complementary view of the Fisher analysis

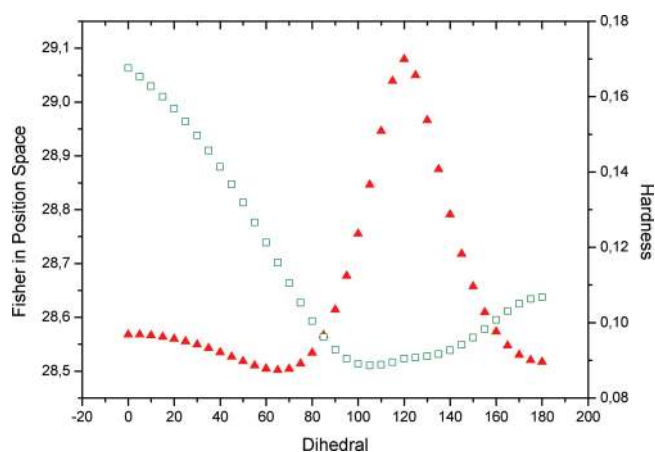


**Figure 4.** Fisher information in position space (red open triangles) and hardness (green open squares) for the vertical eclipsed conformation of ethane as the reference in the vertical case.

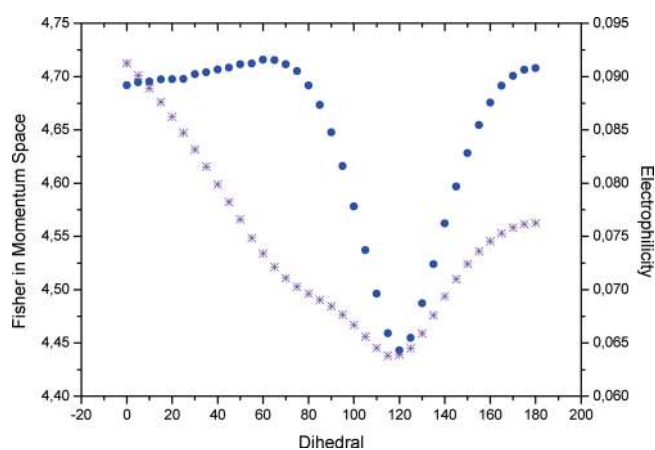


**Figure 5.** Fisher information in momentum space (blue circles) and electrophilicity (cyan asterisks) for the vertical eclipsed conformation of ethane as the reference in the vertical case.

on the distributions in conjugated spaces can be performed in terms of *order/disorder* features (see section 2); i.e., departing from the eclipsed conformation at  $0^\circ$  the disorder in position space augments to reach the staggered conformation around  $60^\circ$  (minimum for the Fisher measure) and as the torsion angle varies a maximum value for the Fisher measure is obtained at  $120^\circ$  when the initial conformeric structure is reached, so that its order is maximum. Then, the disorder increases up to an angle of  $180^\circ$  when the Fisher measure is minimum, indicating that the staggered conformation has been reached.

It is interesting to associate the steric effect with the reactivity parameters, hardness and electrophilicity, through the Fisher information measures. In Figures 4 and 5 we present the values for the hardness and electrophilicity reactivity indexes, which were calculated at the B3LYP/aug-cc-pvdz level. In Figure 4 we have depicted the Fisher information in position space and the hardness for the vertical eclipsed conformation. As mentioned above, hardness represents a measure of the reactivity of a molecule in the sense of the resistance to changes in the electron distribution of the system. Thus, a chemically stable structure holds higher resistance to changes in its electronic distribution corresponding to a higher hardness value and this is reflected in

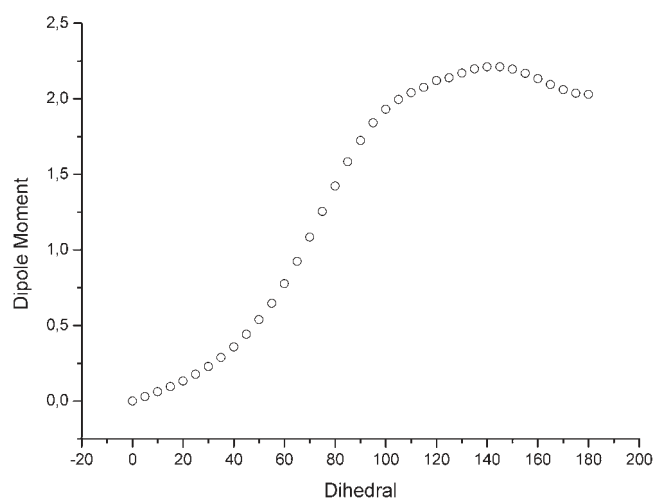


**Figure 6.** Total dipole moment for the eclipsed conformation of ethane as the reference in the vertical case.

the Fisher information measure in position space which possesses lower values for the vertical eclipsed conformer at  $0^\circ$ . In contrast, as the torsion angle varies, hardness values decrease as the hindrance increases, reaching its maximum at  $120^\circ$ , where the larger steric effect is reflected in a lower resistance to changes in the electron density and hence the reactivity of this conformer increases. This is indeed observed in Figure 4, where the hardness attains lower values at the region where Fisher information in position space possesses maximum values, i.e., conformers affected by the steric effect are more reactive and susceptible to changing their corresponding electron distributions.

Figure 5 shows the electrophilicity values for the vertical eclipsed conformation of ethane along with Fisher information in momentum space. It is interesting to note the close resemblance between these quantities, both indicating the same regions, i.e., an inflection point around the staggered conformation ( $60^\circ$ ) and a global minimum at the eclipsed conformation ( $120^\circ$ ). It is apparent that the global electrophilic power of the molecules decreases throughout the conformeric path up to a point where it reaches a minimum at the eclipsed conformer, indicating a structure with the least predisposition to acquire an additional electronic charge because of the steric impediment which is the largest for this conformer (see above), corresponding to a high energy structure with a more delocalized momentum density.

In Figure 6, the total dipole moment for the eclipsed conformation is depicted, which was calculated at the B3LYP/aug-cc-pvdz level. Through the dipole moment we may observe the effect of polarizing the position space density by constraining the geometries as the torsion angle varies. In Figure 6 the total dipole moment is null at  $0^\circ$ , corresponding to the fully relaxed structure of the eclipsed conformation, and then increases up to a point where the torsion angle reaches the conformation with the highest steric effect; hence the total dipole moment reflects the strength of the hindrance impediment caused by the geometry constraints.

**3.2.2. Staggered Conformeric Case.** The total energy for the staggered vertical case at the MP2/aug-ccPVDZ level of theory is depicted in Figure 2, where the conformeric structures were obtained by changing the internal dihedral angle while fixing the rest of the geometric parameters to those of the staggered

optimized conformer. The picture is similar to that of the eclipsed vertical conformer explained above; i.e., as the dihedral angle varies from 180 to 0° the energy remains constant up to a point where the energy reaches a maximum value at 60°, when the staggered conformeric structure is attained. In the absence of other electronic effects arising from the relaxation of the structures, the repulsive energy is mostly caused by the steric effect. Interestingly, this effect is shown to be much more important in the staggered vertical case, with an energy change accounting for as much as 60 hartrees, i.e., 4 times more than the eclipsed vertical case. The physical explanation for this observation is discussed in section 3.2.1.

As in the eclipsed conformeric case, the Fisher information measures in position and momentum spaces for the staggered conformation of ethane were also calculated at the MP2/aug-ccPVDZ level of theory. Although these measures are not depicted, they show a close resemblance with the ones obtained for the eclipsed conformer, except for the fact that the maximum and minimum values for the Fisher measures in position and momentum spaces, respectively, are now observed at 60°. Accordingly, some comments are worth remarking: (i) Fisher measures behave in an opposite manner; (ii) the eclipsed conformation (constrained to the staggered geometry) was observed to be less “compressed” whereas the staggered one is more “squeezed”; (iii) the influence of the steric effect is more pronounced in the staggered conformeric structure. As to the *order/disorder* features of the distributions, we observed that in departing from the staggered conformation at 180° the disorder in position space augments to reach the eclipsed conformation around 120° and as the torsion angle varies a maximum value for the Fisher measure is obtained at 60° when the initial conformeric structure is reached, so that its order is maximum. On the other hand, the behavior of the steric effect for the reference staggered conformation with respect to the reactivity parameters hardness, electrophilicity, and the total dipole moment is analogous to the one analyzed above for the eclipsed case (section 3.2.1). In this case, the extrema for these reactivity properties are found at 60°.

**3.3. Adiabatic Case.** In this section we consider the adiabatic case where the two conformers are in their corresponding optimized structure, along with the rest of the structures at the conformeric path. All of them were calculated at the CCSD(T)/6-311+G\* level of theory for the energy and the Fisher information measures and at the B3LYP/6-311+G\* level for the single point calculations to obtain the reactivity parameters. Densities were obtained with more demanding calculations with a relative error of  $10^{-7}$  for the numerically approximated integrations, in contrast to the vertical cases which do not require highly accurate calculations in order to achieve reliable densities (see discussion below).

The total energy for the adiabatic case is depicted in Figure 1, where the conformeric structures were obtained by relaxing the structures at each point of the path from 0 to 180°. The picture is the standard one, with maxima at 0 and 120° and minima at 60 and 180°. Since the structures are fully optimized, all quantum, steric, and electrostatic<sup>27,30,31</sup> effects are taken into account and we expect the steric effect to be important at the eclipsed conformations according to chemical intuition.

Before proceeding with the analysis of the Fisher information quantities in conjugated spaces, it is worth mentioning that Fisher information in momentum space is especially sensitive to the geometric changes, so in order to achieve reliable results

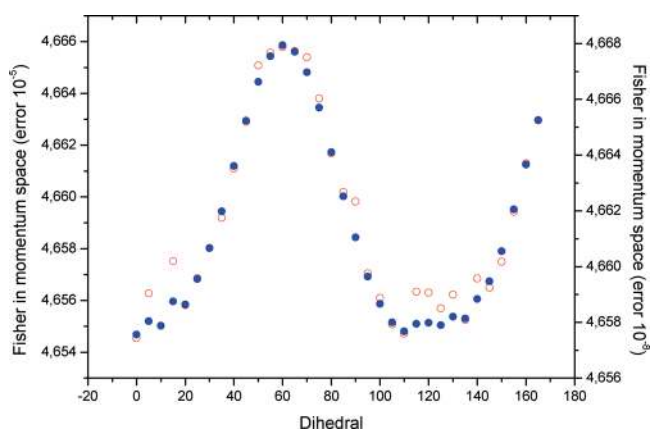


**Figure 7.** Comparison of the Fisher information in position space for the adiabatic conformations of ethane calculated at the HF/6-311+G\* level with a relative error of  $10^{-5}$  (red open circles) and  $10^{-8}$  (blue circles) for the numerically approximated integrations.

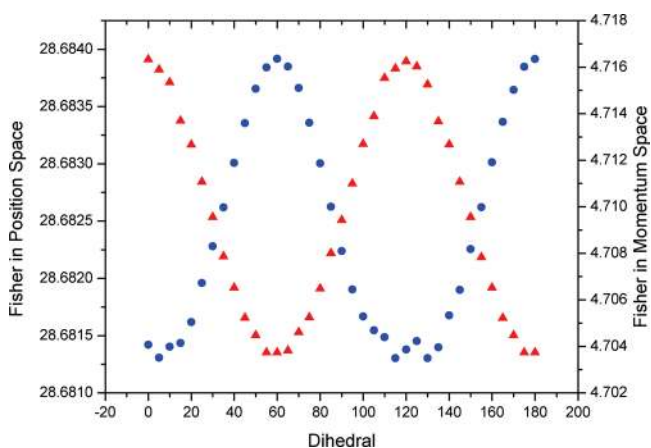


**Figure 8.** Fisher information in conjugated spaces (position space in red triangles; momentum space in blue circles) for the conformational structures of ethane in the adiabatic case.

we had to resort to more demanding criteria for the numerical integrations. As an example we are presenting two different calculations for the Fisher information measures at two different relative errors of  $10^{-5}$  and  $10^{-8}$  for the numerically approximated integrations, both calculated at the HF/6-311+G\* level, which are presented in Figure 7. Since more demanding integration criteria implies very large integration grids (on the order of a million points), the required computing resources become very expensive. Therefore, we decided to set the precision to  $10^{-7}$  in order to obtain acceptable densities within feasible computing capabilities.

Fisher information in position and momentum spaces at the CCSD(T)/6-311+G\* level were calculated with a relative error of  $10^{-7}$ . They are depicted in Figure 8. As in the vertical cases the opposite behavior between these quantities is apparent with Fisher information in position space resembling the profile of the energy (see Figure 1). An information-theoretical analysis performed with Shannon entropies (presented elsewhere<sup>53</sup>) shows that eclipsed conformers at 0 and 120° possess more delocalized densities in both spaces compared with the rest of the conformers; i.e., these structures show higher kinetic energies and



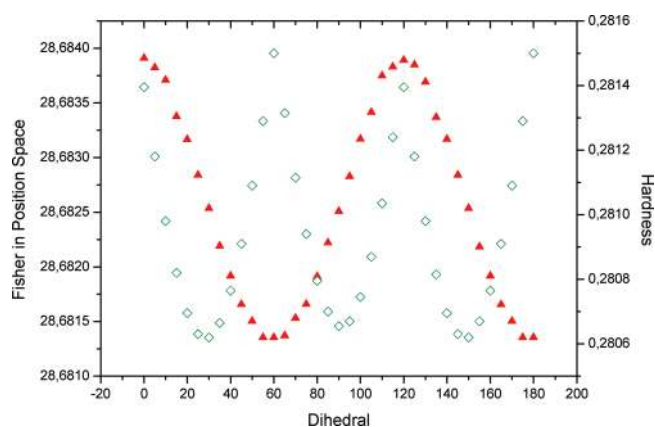


**Figure 9.** Fisher information in position space (red triangles) and hardness (green open tilted squares) for the conformational structures of ethane in the adiabatic case.

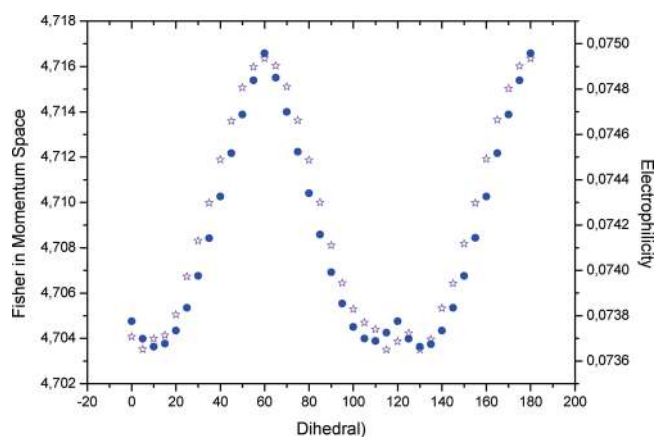


**Figure 10.** Fisher information in momentum space (blue circles) and electrophilicity (cyan stars) for the conformational structures of ethane in the adiabatic case.

hence exert larger steric effects. The situation for the staggered conformers at 60 and 180° is the opposite; i.e., they possess more localized densities in both spaces and their corresponding structures display lower kinetic energies compared with the rest, hence exerting lesser steric effects. The picture for the Fisher information measures are shown in Figure 9, where one may observe that eclipsed conformers hold narrow position densities, affected by steric effects, and less squeezed densities for the staggered conformers. The behavior for the Fisher information measure in momentum space is the opposite, more squeezed momentum densities at the staggered conformers and less narrow ones at the eclipsed conformers, indicating both that eclipsed conformers are prone to suffer steric effects. It is interesting to note that, apparently, Fisher information in momentum space holds more structure at the eclipsed conformations; however, it was difficult to obtain more resolution with the choice of the method and integration criteria. However, it seems from the reactivity parameters (shown below) that there exist indeed more structures around these conformations.

In Figures 9 and 10 we present the values for the hardness and electrophilicity reactivity indexes, which were calculated at the B3LYP/6-311+G\*\*//CCSD(T)/6-311+G\* level. In Figure 9 we have depicted the Fisher information in position space and the

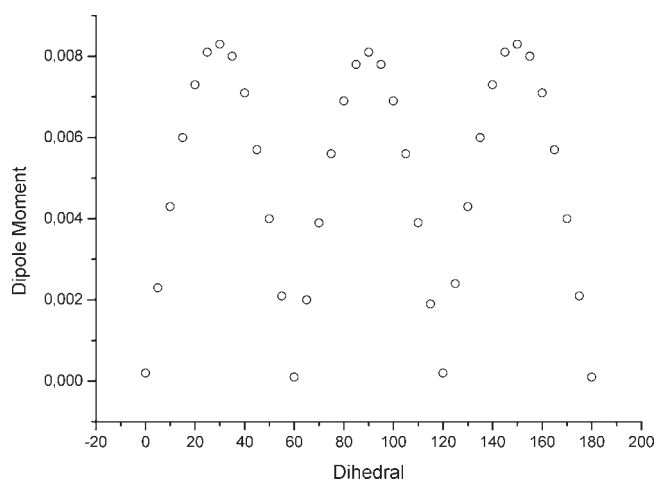


**Figure 11.** Total dipole moment for the conformational structures of ethane in the adiabatic case.

hardness for the adiabatic case. As mentioned above, hardness represents a measure of the reactivity of a molecule in the sense of the resistance to changes in the electron distribution of the system. Thus, we may observe from Figure 9 that hardness attains lower values at 30, 90, and 150° corresponding to intermediate structures, whereas the maxima are attained at the eclipsed and staggered conformations. Interestingly, the maxima are not equal and the largest hardness values correspond to the staggered conformations, indicating larger steric effects for the eclipsed conformations as discussed above.

Figure 10 shows the electrophilicity index for the adiabatic case for ethane along with Fisher information in momentum space. It is interesting to note the close resemblance between both quantities, indicating the same extrema, i.e., minima at 0 and 120° for the eclipsed conformation and maxima at 60 and 180° for the staggered ones. For the former, structures are indicated which show larger steric effects and hence are less susceptible to gaining additional electronic charge. It is interesting to note that electrophilicity index shows more structure around the eclipsed conformers; i.e., a local maximum is clearly observed. This behavior is also manifested in the Fisher measures in momentum space. Therefore, it is apparent that aside from the steric effect there might be other effects (quantum, hyperconjugation, etc.) affecting the local behavior of the momentum density for this conformer.

In Figure 11 the total dipole moment (calculated at the CCSD(T)/6-311+G\* level) is depicted for the adiabatic conformations which is null at the staggered and eclipsed conformers as expected, with maxima at intermediate structures at 30, 90, and 150° in close resemblance to the hardness behavior (see above).

#### 4. CONCLUSIONS

Throughout the study we have performed an information-theoretical analysis of the internal rotation angle of ethane by considering two kinds of rotational barriers: adiabatic, i.e., with optimized geometry, and vertical, i.e., with fixed geometry. Our results show that Fisher information measures in conjugated spaces allow description of the conformeric path of ethane in various situations (adiabatic and vertical) when varying the torsion angle to link the “localized/delocalized” behavior of the distributions with their “narrowness/compression” and hence



with the steric effect. In particular, we find that in the adiabatic case the eclipsed conformer possesses a larger steric repulsion than the staggered conformer for both molecules, but in the vertical cases the staggered conformer retains a larger steric repulsion. Furthermore, we have verified the plausibility of defining and computing the steric effect in the post-Hartree–Fock level of theory according to the density-based quantification scheme proposed by Liu.<sup>27</sup>

## AUTHOR INFORMATION

### Corresponding Author

\*E-mail: esquivel@xanum.uam.mx (R.O.E.); shubin@email.unc.edu (S.L.).

## ACKNOWLEDGMENT

We wish to thank José María Pérez-Jordá and Miroslav Kohout for kindly providing us with their numerical codes. R. O.E. wishes to thank Juan Carlos Angulo and Jesús Sánchez-Dehesa for their kind hospitality during his sabbatical stay at the Departamento de Física Atómica, Molecular y Nuclear and the Instituto Carlos I de Física Teórica y Computacional at the Universidad de Granada, Spain. We acknowledge financial support through Mexican grants from CONACyT, PIFI, and PROMEP-SEP and Spanish grants MICINN projects FIS-2008-02380, FQM-4643, and P06-FQM-2445 of Junta de Andalucía. J.S.D. belongs to the Andalusian research group FQM-207. J.A., J.C.A., and R.O.E. belonged to the Andalusian research group FQM-207 up to January 2011. R.O.E. wishes to acknowledge financial support from the Ministerio de Educación of Spain through Grant SAB2009-0120 and also thanks Prof. Marcelo Galván for his invaluable support and N. Flores-Gallegos for helpful discussions. Allocation of supercomputing time from Laboratorio de Supercómputo y Visualización at UAM, Sección de Supercomputación at CSIRC—Universidad de Granada, and Departamento de Supercómputo at DGSCA-UNAM is gratefully acknowledged.

## REFERENCES

- (1) Fisher, R. A. *Proc. Cambridge Philos. Soc.* **1925**, *22*, 700.
- (2) González-Férez, R.; Dehesa, J. S. *Eur. Phys. J. D.* **2005**, *32*, 39.
- (3) Angulo, J. C.; Antolin, J.; Sen, K. D. *Phys. Lett. A* **2008**, *372*, 670.
- (4) Nalewajski, R. F. *Information Theory of Molecular Systems*; Elsevier Science: New York, 2006.
- (5) Sen, K. D.; Panos, C. P.; Chatzisavvas, K. Ch.; Moustakidis, Ch. C. *Phys. Lett. A* **2007**, *368*, 286.
- (6) Shannon, C. E.; Weaver, W. *The Mathematical Theory of Communication*; University of Illinois Press: Urbana, IL, USA, 1949.
- (7) Tsallis, C. *J. Stat. Phys.* **1988**, *52*, 479.
- (8) Rényi, A. *Proceedings 4th Berkeley Symposium on Mathematics, Statics and Probability*; University of California Press: Berkeley, CA, USA, 1961; Vol. 1; p 547.
- (9) Frieden, B. R. *Science from Fisher Information*; Cambridge University Press: Cambridge, U.K., 2004.
- (10) Cover, T. M.; Thomas, J. A. *Elements of Information Theory*; Wiley-Interscience: Hoboken, NJ, USA, 1991.
- (11) Liu, S. B. *J. Chem. Phys.* **2007**, *126*, 191107.
- (12) Angulo, J. C.; Antolin, J. *J. Chem. Phys.* **2008**, *128*, 164109.
- (13) Panos, C. P.; Chatzisavvas, K. C.; Moustakidis, C. C.; Kyrkou, E. *Phys. Lett. A* **2007**, *363*, 78. Borgoo, A.; de Proft, F.; Geerlings, P.; Sen, K. D. *Chem. Phys. Lett.* **2007**, *444*, 183. Antolin, J.; Angulo, J. C. *Int. J. Quantum Chem.* **2009**, *109*, 586.
- (14) Taneja, I. J.; Pardo, L.; Morales, D.; Menéndez, M. L. *Questiio* **1989**, *13*, 47.
- (15) Kullback, S.; Leibler, A. *Ann. Math. Stat.* **1951**, *22*, 79.
- (16) Antolin, J.; Angulo, J. C.; López-Rosa, S. *J. Chem. Phys.* **2009**, *130*, 074110.
- (17) Lin, J. *IEEE Trans. Inf. Theory* **1991**, *37*, 145.
- (18) Gadre, S. R. *Reviews of Modern Quantum Chemistry: A Celebration of the Contributions of Robert G. Parr*; Sen, K. D., Ed.; World Scientific: Singapore, 2003, Vol. 1, pp 108–147. Koga, T.; Morita, M. *J. Chem. Phys.* **1983**, *79*, 1933. Ghosh, S. K.; Berkowitz, M.; Parr, R. G. *Proc. Natl. Acad. Sci. U.S.A.* **1984**, *81*, 8028. Angulo, J. C.; Dehesa, J. S. *J. Chem. Phys.* **1992**, *97*, 6485. Massen, S. E.; Panos, C. P. *Phys. Lett. A* **1998**, *246*, 530. Nalewajski, R. F.; Parr, R. G. *J. Phys. Chem. A* **2001**, *105*, 7391. Nagy, A. *J. Chem. Phys.* **2003**, *119*, 9401. Romera, E.; Dehesa, J. S. *J. Chem. Phys.* **2004**, *120*, 8906. Karafiloglou, P.; Panos, C. P. *Chem. Phys. Lett.* **2004**, *389*, 400. Sen, K. D. *J. Chem. Phys.* **2005**, *123*, 074110. Parr, R. G.; Nalewajski, R. F.; Ayers, P. W. *J. Phys. Chem. A* **2005**, *109*, 3957. Guevara, N. L.; Sagar, R. P.; Esquivel, R. O. *J. Chem. Phys.* **2005**, *122*, 084101. Shi, Q.; Kais, S. *J. Chem. Phys.* **2005**, *309*, 127. Chatzisavvas, K. Ch.; Moustakidis, Ch. C.; Panos, C. P. *J. Chem. Phys.* **2005**, *123*, 174111. Sen, K. D.; Katriel, J. *J. Chem. Phys.* **2006**, *125*, 074117. Nagy, A. *Chem. Phys. Lett.* **2006**, *425*, 154. Ayers, P. W. *Theor. Chem. Acc.* **2006**, *115*, 253. Martysheva, L. M.; Seleznev, V. D. *Phys. Rep.* **2006**, *426*, 1. Liu, S. *J. Chem. Phys.* **2007**, *126*, 191107. Borgoo, A.; Jaque, P.; Toro-Labbé, A.; Van Alsenoy, Ch.; Geerlings, P. *Phys. Chem. Chem. Phys.* **2009**, *11*, 476.
- (19) Esquivel, R. O.; Flores-Gallegos, N.; Iuga, C.; Carrera, E.; Angulo, J. C.; Antolin, J. *Theor. Chem. Acc.* **2009**, *124*, 445–460.
- (20) Esquivel, R. O.; Flores-Gallegos, N.; Iuga, C.; Carrera, E.; Angulo, J. C.; Antolin, J. *Phys. Lett. A* **2010**, *374*, 948–951.
- (21) López-Rosa, S.; Esquivel, R. O.; Angulo, J. C.; Antolin, J.; Dehesa, J. S.; Flores-Gallegos, N. *J. Chem. Theory Comput.* **2010**, *6*, 145–154.
- (22) Esquivel, R. O.; Angulo, J. C.; Antolin, J.; Dehesa, J. S.; López-Rosa, S.; Flores-Gallegos, N. *Phys. Chem. Chem. Phys.* **2010**, *12*, 7108–7116.
- (23) Wyatt, R. E.; Parr, R. G. *J. Chem. Phys.* **1965**, *43*, 217. Wyatt, R. E.; Parr, R. G. *J. Chem. Phys.* **1966**, *44*, 1529. Zaalberg, M. M. *Theor. Chim. Acta* **1966**, *5*, 79.
- (24) Fadiel, A.; Eichenbaum, K. D.; Hamza, A.; Tan, O.; Lee, H. H.; Naftolin, F. *Curr. Protein Pept. Sci.* **2007**, *8*, 29.
- (25) Kufer, T. A. *Mol. Biosyst.* **2008**, *4*, 380. Levine, A. J.; Hu, W. W.; Feng, Z. H.; Gil, G. *Ann. N. Y. Acad. Sci.* **2007**, *1115*, 32.
- (26) Mo, Y. R.; Gao, J. L. *Acc. Chem. Res.* **2007**, *40*, 113. Bickelhaupt, F. M.; Baerends, E. J. *Angew. Chem., Int. Ed.* **2003**, *42*, 4183. Baerends, E. J. *Nachr. Chem.* **2004**, *52*, 581. Grunenberg, J. *Nachr. Chem.* **2004**, *52*, 831. Mo, Y. R.; Wu, W.; Song, L. C.; Lin, M. H.; Zhang, Q.; Gao, J. L. *Angew. Chem., Int. Ed.* **2004**, *43*, 1986. Schreiner, P. *Nachr. Chem.* **2004**, *52*, 581. Sadlej-Sosnowska, N. *J. Phys. Chem. A* **2003**, *107*, 8671. Goodman, L.; Pophristic, V.; Wang, W. *Int. J. Quantum Chem.* **2002**, *90*, 657. Schreiner, P. R. *Angew. Chem., Int. Ed.* **2002**, *41*, 3579. Pophristic, V.; Goodman, L. *Nature (London)* **2001**, *411*, S65.
- (27) Liu, S. B. *J. Chem. Phys.* **2007**, *126*, 244103.
- (28) Nagy, A. *Chem. Phys. Lett.* **2007**, *449*, 212.
- (29) Torrent-Sucarrat, M.; Liu, S.; De Proft, F. *J. Phys. Chem. A* **2009**, *113*, 3698.
- (30) Liu, S. B.; Govind, N. *J. Phys. Chem. A* **2008**, *112*, 6690.
- (31) Liu, S. B.; Govind, N.; Pedersen, L. G. *J. Chem. Phys.* **2008**, *129*, 094104.
- (32) Liu, S. B.; Hao, H.; Pedersen, L. G. *J. Phys. Chem. A* **2010**, *114*, 5913.
- (33) Rawlings, D. C.; Davison, E. R. *J. Phys. Chem.* **1985**, *89*, 969.
- (34) Kaijser, P.; Smith, V. H., Jr. *Adv. Quantum Chem.* **1997**, *10*, 37.
- (35) Kohout, M. Program DGRID, version 4.2, 2007.
- (36) Hamilton, I. P.; Mosna, R. A. *J. Comput. Appl. Math.* **2010**, *233*, 1542. DOI: 10.1016/j.cam.2009.02.087.
- (37) Dehesa, J. S.; Gonzalez-Ferez, R.; Sanchez-Moreno, P. *J. Phys. A: Math. Theor.* **2011**, *44*, 065301.

- (38) von Weizsäcker, C. F. *Z. Phys.* **1935**, *96*, 431.
- (39) Dembo, A.; Cover, T. A.; Thomas, J. A. *IEEE Trans. Inf. Theory* **1991**, *32*, 1501.
- (40) Koopmans, T. A. *Physica* **1933**, *1*, 104.
- (41) Parr, R. G.; Yang, W. *Density-Functional Theory of Atoms and Molecules*; Oxford University Press: New York, 1989.
- (42) Parr, R. G.; Pearson, R. G. *J. Am. Chem. Soc.* **1983**, *105*, 7512.
- (43) Ayers, P. W.; Parr, R. G.; Pearson, R. G. *J. Chem. Phys.* **2006**, *124*, 194107. Pearson, R. G. *Inorg. Chim. Acta* **1995**, *240*, 93.
- (44) Geerlings, P.; De Proft, F.; Langenaeker, W. *Chem. Rev.* **2003**, *103*, 1793.
- (45) Ghanty, T. K.; Ghosh, S. K. *J. Phys. Chem.* **1993**, *97*, 4951. Roy, R.; Chandra, A. K.; Pal, S. J. *Phys. Chem.* **1994**, *98*, 10447. Hati, S.; Datta, D. J. *Phys. Chem.* **1994**, *98*, 10451. Simon-Manso, Y.; Fuentealba, P. *J. Phys. Chem. A* **1998**, *102*, 2029.
- (46) Chattaraj, P. K.; Sarkar, U.; Roy, D. R. *Chem. Rev.* **2006**, *106*, 2065.
- (47) Pearson, R. G. *J. Am. Chem. Soc.* **1963**, *85*, 3533. Pearson, R. G. *Hard and Soft Acids and Bases*; Dowden, Hutchinson and Ross: Stroudsburg, PA, USA, 1973. Pearson, R. G. *Chemical Hardness*; Wiley-VCH: New York, 1997.
- (48) Parr, R. G.; Szentpály, L. V.; Liu, S. J. *Am. Chem. Soc.* **1999**, *121*, 1922.
- (49) Hariharan, P. C.; Pople, J. A. *Theor. Chim. Acta* **1973**, *28*, 213. Francl, M. M.; Pietro, W. J.; Henre, W. J.; Binkley, J. S.; Gordon, M. S.; DeFrees, D. J.; Pople, J. A. *J. Chem. Phys.* **1982**, *77*, 3654.
- (50) Dunning, T. H. *J. Chem. Phys.* **1989**, *90*, 1007.
- (51) Frisch, M. J.; Trucks, G. W.; Schlegel, H. B.; Scuseria, G. E.; Robb, M. A.; Cheeseman, J. R.; Montgomery, J. A., Jr.; Vreven, T.; Kudin, K. N.; Burant, J. C.; Millam, J. M.; Iyengar, S. S.; Tomasi, J.; Barone, V.; Mennucci, B.; Cossi, M.; Scalmani, G.; Rega, N.; Petersson, G. A.; Nakatsuji, H.; Hada, M.; Ehara, M.; Toyota, K.; Fukuda, R.; Hasegawa, J.; Ishida, M.; Nakajima, T.; Honda, Y.; Kitao, O.; Nakai, H.; Klene, M.; Li, X.; Knox, J. E.; Hratchian, H. P.; Cross, J. B.; Bakken, V.; Adamo, C.; Jaramillo, J.; Gomperts, R.; Stratmann, R. E.; Yazyev, O.; Austin, A. J.; Cammi, R.; Pomelli, C.; Ochterski, J. W.; Ayala, P. Y.; Morokuma, K.; Voth, G. A.; Salvador, P.; Dannenberg, J. J.; Zakrzewski, V. G.; Dapprich, S.; Daniels, A. D.; Strain, M. C.; Farkas, O.; Malick, D. K.; Rabuck, A. D.; Raghavachari, K.; Foresman, J. B.; Ortiz, J. V.; Cui, Q.; Baboul, A. G.; Clifford, S.; Cioslowski, J.; Stefanov, B. B.; Liu, G.; Liashenko, A.; Piskorz, P.; Komaromi, I.; Martin, R. L.; Fox, D. J.; Keith, T.; Al-Laham, M. A.; Peng, C. Y.; Nanayakkara, A.; Challacombe, M.; Gill, P. M. W.; Johnson, B.; Chen, W.; Wong, M. W.; Gonzalez, C.; Pople, J. A. *Gaussian 03*, revision D.01; Gaussian, Inc.: Wallingford, CT, USA, 2004.
- (52) Pérez-Jordá, J. M.; San-Fabián, E. *Comput. Phys. Commun.* **1993**, *77*, 46. Pérez-Jordá, J. M.; Becke, A. D.; San-Fabián, E. *J. Chem. Phys.* **1994**, *100*, 6520.
- (53) Esquivel, R. O.; Angulo, J. C.; Liu, S. B.; Dehesa, J. S.; Antolin, J.; Molina-Espíritu, M. Manuscript in preparation, 2011.